



Observation of a charmonium-like enhancement in the $\gamma\gamma \rightarrow \omega J/\psi$ process

S. Uehara,⁹ T. Aushev,^{20,14} A. M. Bakich,³⁹ K. Belous,¹² V. Bhardwaj,³⁵ M. Bischofberger,²⁶ M. Bračko,^{22,15} T. E. Browder,⁸ P. Chang,²⁹ A. Chen,²⁷ P. Chen,²⁹ B. G. Cheon,⁷ C.-C. Chiang,²⁹ I.-S. Cho,⁴⁸ S.-K. Choi,⁶ Y. Choi,³⁸ J. Dalseno,^{23,41} A. Drutskoy,³ S. Eidelman,^{1,33} D. Epifanov,^{1,33} M. Feindt,¹⁷ N. Gabyshev,^{1,33} H. Ha,¹⁸ J. Haba,⁹ K. Hayasaka,²⁵ H. Hayashii,²⁶ Y. Hoshi,⁴³ W.-S. Hou,²⁹ Y. B. Hsiung,²⁹ H. J. Hyun,¹⁹ K. Inami,²⁵ R. Itoh,⁹ M. Iwabuchi,⁴⁸ M. Iwasaki,⁴⁴ Y. Iwasaki,⁹ N. J. Joshi,⁴⁰ J. H. Kang,⁴⁸ T. Kawasaki,³² C. Kiesling,²³ H. J. Kim,¹⁹ J. H. Kim,³⁸ Y. I. Kim,¹⁹ Y. J. Kim,⁵ B. R. Ko,¹⁸ P. Kodyš,² S. Korpar,^{22,15} P. Krizan,^{21,15} P. Krokovny,⁹ T. Kumita,⁴⁵ A. Kuzmin,^{1,33} Y.-J. Kwon,⁴⁸ S.-H. Kyeong,⁴⁸ J. S. Lange,⁴ M. J. Lee,³⁷ S.-H. Lee,¹⁸ J. Li,⁸ C. Liu,³⁶ Y. Liu,²⁵ D. Liventsev,¹⁴ R. Louvot,²⁰ A. Matyja,³⁰ S. McOnie,³⁹ K. Miyabayashi,²⁶ H. Miyata,³² Y. Miyazaki,²⁵ R. Mizuk,¹⁴ R. Mussa,¹³ E. Nakano,³⁴ M. Nakao,⁹ H. Nakazawa,²⁷ Z. Natkaniec,³⁰ S. Nishida,⁹ O. Nitoh,⁴⁶ S. Ogawa,⁴² T. Ohshima,²⁵ S. Okuno,¹⁶ S. L. Olsen,^{37,8} P. Pakhlov,¹⁴ G. Pakhlova,¹⁴ C. W. Park,³⁸ H. Park,¹⁹ H. K. Park,¹⁹ R. Pestotnik,¹⁵ M. Petrič,¹⁵ L. E. Piilonen,⁴⁷ M. Röhrken,¹⁷ S. Ryu,³⁷ H. Sahoo,⁸ Y. Sakai,⁹ O. Schneider,²⁰ C. Schwanda,¹¹ M. E. Sevier,²⁴ M. Shapkin,¹² C. P. Shen,⁸ J.-G. Shiu,²⁹ B. Shwartz,^{1,33} J. B. Singh,³⁵ P. Smerkol,¹⁵ E. Solovieva,¹⁴ M. Starič,¹⁵ Y. Teramoto,³⁴ K. Trabelsi,⁹ Y. Unno,⁷ S. Uno,⁹ P. Urquijo,²⁴ G. Varner,⁸ K. Vervink,²⁰ C. H. Wang,²⁸ P. Wang,¹⁰ Y. Watanabe,¹⁶ R. Wedd,²⁴ E. Won,¹⁸ B. D. Yabsley,³⁹ Y. Yamashita,³¹ C. Z. Yuan,¹⁰ C. C. Zhang,¹⁰ T. Zivko,¹⁵ and O. Zyukova,^{1,33}

(The Belle Collaboration)

¹*Budker Institute of Nuclear Physics, Novosibirsk*

²*Faculty of Mathematics and Physics, Charles University, Prague*

³*University of Cincinnati, Cincinnati, Ohio 45221*

⁴*Justus-Liebig-Universität Gießen, Gießen*

⁵*The Graduate University for Advanced Studies, Hayama*

⁶*Gyeongsang National University, Chinju*

⁷*Hanyang University, Seoul*

⁸*University of Hawaii, Honolulu, Hawaii 96822*

⁹*High Energy Accelerator Research Organization (KEK), Tsukuba*

¹⁰*Institute of High Energy Physics, Chinese Academy of Sciences, Beijing*

¹¹*Institute of High Energy Physics, Vienna*

¹²*Institute of High Energy Physics, Protvino*

¹³*INFN - Sezione di Torino, Torino*

¹⁴*Institute for Theoretical and Experimental Physics, Moscow*

¹⁵*J. Stefan Institute, Ljubljana*

¹⁶*Kanagawa University, Yokohama*

¹⁷*Institut für Experimentelle Kernphysik, Karlsruhe Institut für Technologie, Karlsruhe*

¹⁸*Korea University, Seoul*

¹⁹*Kyungpook National University, Taegu*

²⁰*École Polytechnique Fédérale de Lausanne (EPFL), Lausanne*

²¹*Faculty of Mathematics and Physics, University of Ljubljana, Ljubljana*

²²*University of Maribor, Maribor*

²³*Max-Planck-Institut für Physik, München*

²⁴*University of Melbourne, School of Physics, Victoria 3010*

²⁵*Nagoya University, Nagoya*

²⁶*Nara Women's University, Nara*

²⁷*National Central University, Chung-li*

²⁸*National United University, Miao Li*

²⁹*Department of Physics, National Taiwan University, Taipei*

³⁰*H. Niewodniczanski Institute of Nuclear Physics, Krakow*

³¹*Nippon Dental University, Niigata*

³²*Niigata University, Niigata*

³³*Novosibirsk State University, Novosibirsk*

³⁴*Osaka City University, Osaka*

³⁵*Panjab University, Chandigarh*

³⁶University of Science and Technology of China, Hefei

³⁷Seoul National University, Seoul

³⁸Sungkyunkwan University, Suwon

³⁹School of Physics, University of Sydney, NSW 2006

⁴⁰Tata Institute of Fundamental Research, Mumbai

⁴¹Excellence Cluster Universe, Technische Universität München, Garching

⁴²Toho University, Funabashi

⁴³Tohoku Gakuin University, Tagajo

⁴⁴Department of Physics, University of Tokyo, Tokyo

⁴⁵Tokyo Metropolitan University, Tokyo

⁴⁶Tokyo University of Agriculture and Technology, Tokyo

⁴⁷IPNAS, Virginia Polytechnic Institute and State University, Blacksburg, Virginia 24061

⁴⁸Yonsei University, Seoul

We report the results of a search for a charmonium-like state produced in the process $\gamma\gamma \rightarrow \omega J/\psi$ in the 3.9–4.2 GeV/ c^2 mass region. We observe a significant enhancement, which is well-described by a resonant shape with mass $M = (3915 \pm 3 \pm 2)$ MeV/ c^2 and total width $\Gamma = (17 \pm 10 \pm 3)$ MeV. This enhancement may be related to one or more of the three charmonium-like states so far reported in the 3.90–3.95 GeV/ c^2 mass region.

PACS numbers: 13.25.Gv, 13.66.Bc, 14.40.Pq, 14.40.Rt

Many new charmonium-like states have been discovered by the B-factory experiments, typically via a prominent hadronic decay to a known charmonium state, such as J/ψ , $\psi(2S)$ or χ_{c1} . Some have attracted particular interest because of their net electric charge [1]. Three of the new (neutral) states were discovered by Belle in the 3.90–3.95 GeV/ c^2 mass region. The $X(3940)$ was found in the $e^+e^- \rightarrow J/\psi X$ double charmonium production process, with a prominent decay to the $D\bar{D}^*$ final state [2]. The $Y(3940)$ was observed in the B decay process $B^- \rightarrow Y(3940)K^-$ with $Y(3940) \rightarrow \omega J/\psi$ [3, 4], and is a candidate for an exotic state, such as a hybrid meson ($c\bar{c}g$), or a $D^*\bar{D}^*$ bound state [5]. The $Z(3930)$ was found in the $\gamma\gamma \rightarrow D\bar{D}$ process [6], and is usually identified with the $\chi_{c2}(2P)$. These three states appear in different production and decay processes, and are usually considered to be distinct particles, however there is no decisive evidence for this. The interpretation of these states has been discussed by many authors: see, *e.g.*, Ref. [7].

It is important to search for a signature of the $Y(3940)$ or any other resonant state contributing to two-photon production of $\omega J/\psi$. This final state is the lightest combination of two vector mesons with definite C -even and $I = 0$ quantum numbers that can be produced in two-photon processes via a hidden-charm state. In this paper we present measurements of the $\gamma\gamma \rightarrow \omega J/\psi$ process in the 3.9–4.2 GeV/ c^2 mass region, in which we observe a resonant enhancement. The signal is from the two-photon process $e^+e^- \rightarrow e^+e^-\omega J/\psi$ in the “zero-tag” mode, where neither the final-state electron nor positron recoiling from photon emission are detected.

We use experimental data recorded with the Belle detector [8] at the KEKB e^+e^- asymmetric-energy (3.5 on 8 GeV) collider [9], corresponding to an integrated luminosity of 694 fb $^{-1}$. The data are accumulated mainly

on the $\Upsilon(4S)$ resonance ($\sqrt{s} = 10.58$ GeV) and 60 MeV below it. A small fraction of data from different beam energies near 10.36 GeV (the $\Upsilon(3S)$ mass) and 10.87 GeV (the $\Upsilon(5S)$ mass) is also included in the sample.

A comprehensive description of the Belle detector is given elsewhere [8]. Charged tracks are reconstructed in a central drift chamber (CDC) located in a uniform 1.5 T solenoidal magnetic field. The z axis of the detector and the solenoid is along the positron beam, with the positrons moving in the $-z$ direction. Track trajectory coordinates near the collision point are measured by a silicon vertex detector (SVD). Photon detection and energy measurements are provided by a CsI(Tl) electromagnetic calorimeter (ECL). A combination of silica-aerogel Cherenkov counters (ACC), a time-of-flight counter (TOF) system consisting of a barrel of 128 plastic scintillation counters, and specific ionization (dE/dx) measurements in the CDC provides K/π separation for charged tracks over a wide momentum range. The magnet return iron is instrumented to form a K_L detection and muon identification (KLM) system that detects muon tracks.

Signal candidates are triggered by a variety of track triggers that require two or more CDC tracks associated with TOF hits, ECL clusters, a total energy deposit in the ECL above a threshold (0.5 GeV), or a muon track in the KLM detector. In addition, events with a total ECL energy above 1.1 GeV are triggered by a separate logic. Because of the presence of a lepton pair in the final state of the signal processes, a combination of the above triggers provides a high overall trigger efficiency, $(98 \pm 2)\%$.

We select signal event candidates by reconstructing all the final state particles from $\omega \rightarrow \pi^+\pi^-\pi^0$ and $J/\psi \rightarrow l^+l^-$ ($l = e$ or μ). Twelve selection criteria are imposed: (1) there are just 4 charged tracks with trans-

verse momentum $p_t > 0.1$ GeV/c originating in the beam collision region; (2) the net charge of the tracks is zero; (3) none of the tracks is identified as a kaon (we require a likelihood ratio $\mathcal{L}(K)/(\mathcal{L}(K) + \mathcal{L}(\pi)) < 0.8$, which is satisfied by 99.6% of pions but only 5% of kaons, for momenta below 0.8 GeV/c); (4) there is a net-charge-zero combination of two tracks whose invariant mass is in the J/ψ mass region, $|M(2 \text{ tracks}) - M_{J/\psi}| < 0.2$ GeV/ c^2 , where $M_{J/\psi} = 3.0969$ GeV/ c^2 and we assume the pion mass for each of the two tracks; (5) there is one or more neutral pion candidate formed by a mass-constrained fit of two photons, with $\chi^2 < 4$; (6) the number of π^0 's with $p_t > 0.1$ GeV/c must not exceed one in an event. If there is a π^0 satisfying the p_t condition, it is accepted as the only π^0 candidate in that event. If no π^0 satisfies the p_t condition, we retain all the π^0 candidates (below $p_t < 0.1$ GeV/c) at this stage; (7) events in the kinematic region of initial-state-radiation processes, $e^+e^- \rightarrow \gamma X$, where the photon is emitted very close to the direction of the incident e^- beam, are eliminated. We reject events satisfying the following condition on the z -component of the laboratory momentum for the final-state system X , $P_z < (M_5^2 - 49.0 \text{ GeV}^2/c^4)/14.0 \text{ GeV}/c^3 + 0.6 \text{ GeV}/c$, where P_z and M_5 are the z -component of the momentum and the invariant mass of the system constructed from the four tracks and a neutral pion candidate, respectively.

For further analysis we examine only events with $W < 4.3$ GeV, where W is defined by $W = M_5 - M(l^+l^-) + M_{J/\psi}$, using a refined two-lepton invariant mass ($M(l^+l^-)$) based on the lepton flavor identified by the following criteria: (8) if either of the tracks is identified as an electron, based on the ECL energy deposit, the tracks are identified as e^+e^- . Otherwise, if either track is identified as a muon based on KLM information, the tracks are identified as $\mu^+\mu^-$. An event that fails both tests is rejected. If one or more photons with energy between 20 and 200 MeV are found within 3° of either the e^+ or e^- track, the energy of the most energetic photon near the track is added to the track momentum.

Following this correction, (9) we refine the J/ψ selection with a more stringent requirement for the lepton-pair invariant mass, $3.07 \text{ GeV}/c^2 < M(l^+l^-) < 3.12 \text{ GeV}/c^2$; (10) we suppress $\psi(2S)\pi^0$ events with the mass difference requirement, $|M(l^+l^-\pi^+\pi^-) - M(l^+l^-) - 0.589 \text{ GeV}/c^2| > 0.01 \text{ GeV}/c^2$; (11) to select ω candidate, a condition on the $\pi^+\pi^-\pi^0$ invariant mass, $0.753 \text{ GeV}/c^2 < M(3\pi) < 0.813 \text{ GeV}/c^2$, is imposed. If there are multiple ω candidates due to multiple π^0 's in an event, we choose the one with the smallest χ^2 in the π^0 mass constrained fit, in order to avoid multiple entries in the final $\omega J/\psi$ mass spectrum. Finally, (12) we require transverse momentum balance for the 5-body system, $|\sum \mathbf{p}_t^*| < 0.1 \text{ GeV}/c$, where \mathbf{p}_t^* is the momentum of a particle in the e^+e^- c.m. frame, in the plane perpendicular to the beam direction [10].

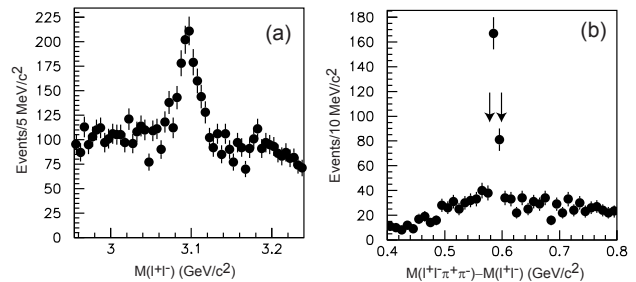


FIG. 1: (a) The $M(l^+l^-)$ distribution just after the dilepton selection. (b) The $M(l^+l^-\pi^+\pi^-) - M(l^+l^-)$ distribution after the tight J/ψ selection. Events between the arrows are rejected as consistent with $\psi(2S)$ production.

Figures 1(a) and 1(b) show the distributions of $M(l^+l^-)$ just after requirement (8) and the mass difference $M(l^+l^-\pi^+\pi^-) - M(l^+l^-)$ just after requirement (9), respectively. The $\psi(2S)$ contribution is effectively removed by criterion (10) above.

The main background process is multi-pion production from two-photon processes. However, after all selection requirements are applied, non- $\omega J/\psi$ backgrounds are rather small, as shown in the scatter plot in Fig. 2(a) for the samples where all the selections except those for $M(l^+l^-)$ and $M(3\pi)$ are applied. Figures 2(b) and 2(c) show the distributions of $M(l^+l^-)$ and $M(3\pi)$, respectively, in the selection bands for the opposite-side particle; for clarity, we exclude events somewhat below the $\omega J/\psi$ threshold, $W \leq 3.85$ GeV.

In Figs. 2(b) and 2(c), the experimental $M(l^+l^-)$ and $M(3\pi)$ distributions are compared with those from the signal Monte Carlo (MC) events, which are generated assuming spin-parity (J^P) and mass (W) of the $\omega J/\psi$ system to be 0^+ and 3.93 GeV/ c^2 , respectively. Details of the signal MC generation are given below. We confirm that the experimental mass distributions are consistent with those of signal MC events.

We find that there are two events in the signal region with multiple ω candidates, out of 73 events in total; we choose only one combination in each event, according to criterion (11). The fraction is consistent with the 1–2% multiple candidate rate expected from the signal MC sample.

We show the W distribution for the final $\gamma\gamma \rightarrow \omega J/\psi$ candidate events in Fig. 3. There is a prominent resonance-like peak around 3.92 GeV. It is far above the non- $\omega J/\psi$ background contribution, which is estimated from the events in the ω and J/ψ mass sidebands (shown as shaded histograms for comparison); we define eight sideband regions in the plane of Fig. 2(a) with the same dimensions as the signal region, *i.e.*, each region centered at 3.035 GeV, 3.095 GeV or 3.155 GeV with a width of 0.05 GeV in the $M(l^+l^-)$ direction and centered at 0.693 GeV, 0.783 GeV and 0.873 GeV with a width of 0.06 GeV in the $M(3\pi)$ direction, and average the dis-

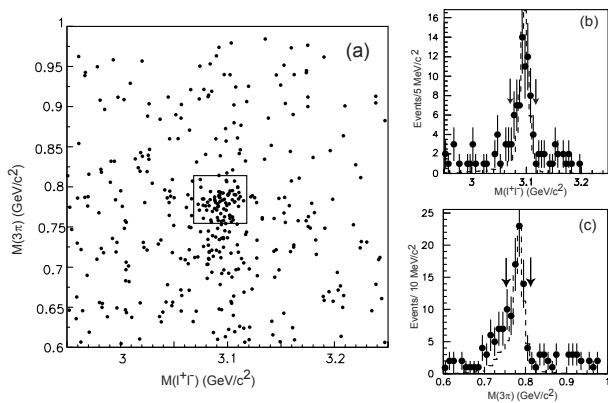


FIG. 2: (a) Scatter plot of $M(3\pi)$ vs. $M(l^+l^-)$ for the experimental data, with all the other cuts applied. The rectangle shows the signal region. (b) The $M(l^+l^-)$ and (c) $M(3\pi)$ distributions with all the other cuts applied, and requiring $W > 3.85$ GeV. Entries due to multiple ω candidates in a given event are included. Points with error bars show the data; the dashed histograms show signal MC events, normalized to the data yield in the selection area, with the scaled sideband yield subtracted. The arrows show the selection regions.

tribution over the eight regions. We modify the W value of each sideband event plotted in Fig. 3, shifting it by the difference between the sum of mass coordinates of the central point of the signal region (3.878 GeV) from that of the sideband region where the event is found, for comparison to the signal-event distribution.

Figure 4(a) shows a scatter plot of the transverse momentum balance vs. W after requirement (11). A prominent concentration of events near $W = 3.89 - 3.95$ GeV and $|\sum \mathbf{p}_t^*| < 0.05$ GeV/c is visible; a comparison of the $|\sum \mathbf{p}_t^*|$ projection with signal MC is shown in Fig. 4(b). Based on these results, and the shape in W (Fig. 3), we conclude that the concentration of events is due to a resonance formed in two-photon collisions.

The W distribution for the final candidate events is fitted by an incoherent sum of resonant and background components. We adopt an S-wave Breit-Wigner function with a variable width for the resonant component, $(2N_R/\pi)M^2\Gamma'/\{(W^2 - M^2)^2 + M^2\Gamma'^2\}$ and $\Gamma' = \Gamma(p^*/p_0^*)$, where p^* is the momentum of the two-body decay to $\omega J/\psi$, in the rest frame of a parent particle of mass W ; p_0^* is the value for $W = M$ [3]. The nominal mass (M), width (Γ) and yield parameter (N_R) are treated as fit parameters.

We represent the background component by a quadratic function of p^* that vanishes at the nominal $\omega J/\psi$ threshold, $M_{\text{th}} = 3.8796$ GeV/c^2 . We also add a constant term, to represent the high W tail, which, as the sideband study suggests, is dominated by non- $\omega J/\psi$ events. The sum of the two components has a functional form, $\{(ap^* + bp^{*2}) + c\}\theta(W - M_{\text{th}})$, where $\theta(x)$ is a unit step function that is non-zero only for $x > 0$. The param-

eters a , b and c are floated within the constraint that each of the two background components must be non-negative throughout the fitting region.

The fit takes into account the W resolution in the measurement, which is approximated by a double-Gaussian function from the signal MC events (59% of the signal has a resolution σ of 4.5 MeV, while the remainder has $\sigma = 16$ MeV with the peak position displaced by -4 MeV). We perform an unbinned maximum likelihood fit in the region $3.875 \text{ GeV} < W < 4.2$ GeV. The signal candidates with the smallest W are the two events with W between 3.879 and 3.880 GeV.

The W dependences of the efficiency and luminosity function are taken into account in the fitting function. The efficiency is determined using signal MC events as described in detail later. We use the W dependence of the efficiency for $J^P = 0^+$ for the nominal fit. Between the threshold and 3.96 GeV, the W -dependence is weak: the efficiency varies by 10% only, and has a minimum near $W = 3.92$ GeV.

The obtained resonance parameters for the mass and the width are as follows:

$$\begin{aligned} M &= (3915 \pm 3 \pm 2) \text{ MeV}/c^2, \\ \Gamma &= (17 \pm 10 \pm 3) \text{ MeV}, \end{aligned}$$

where the first and second errors are statistical and systematic, respectively. The estimated yield from the resonant component in the fit is $49 \pm 14 \pm 4$ events in the region below 4.2 GeV. The statistical significance of the resonant peak is 7.7σ , which is determined from the difference of the logarithmic likelihoods, $-2\ln(L/L_0)$, taking the difference of the number of degrees of freedom in the fits into account, where L_0 and L are the likelihoods of the fits with and without a resonant component, respectively. The relevant fit curves are shown in Fig. 3. The χ^2 of the nominal fit, determined using 10-MeV-width binning in the range 3.85–4.2 GeV, is 27.3, for 29 degrees of freedom.

The systematic errors quoted above are determined from a study of alternate fits: we use a Breit-Wigner function with a constant width; we enlarge the invariant-mass resolution by 20% (an over-estimate of the data-Monte Carlo difference allowed by the fit); we change the upper limit of the fit region in W to 4.1 GeV and 4.3 GeV, respectively. The changes in the central values of the corresponding resonance parameter are combined in quadrature. We also take into account the uncertainty of the mass scale, estimated to be 1 MeV/c^2 , in the measurement of M . There is no significant change in the parameters if $J^P = 2^+$ is assumed; the changes of mass and width are less than 0.1 MeV/c^2 and 0.3 MeV, respectively. The resonant contribution for the $J^P = 2^+$ assumption is 1.0 event smaller than that for $J^P = 0^+$.

The efficiency for selecting $\gamma\gamma \rightarrow \omega J/\psi$ events is determined using signal MC events generated by TREPS

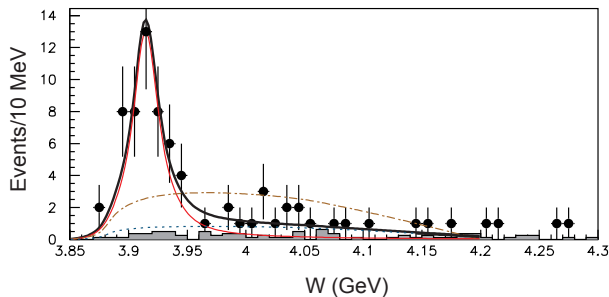


FIG. 3: The W distribution of the final candidate events (dots with error bars). The shaded histogram is the distribution of non- $\omega J/\psi$ backgrounds estimated from the sideband distributions. The bold solid, thinner solid and dashed curves are the total, resonance and background contributions, respectively, from the standard fit (see the text). The dot-dashed curve is the fit without a resonance.

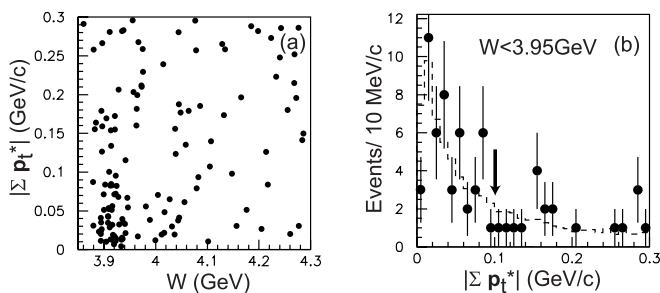


FIG. 4: (a) Scatter plot of p_t balance *vs.* W for the final candidate events in which only requirement (12) is omitted. (b) The projection onto the p_t balance axis for events with $W < 3.95$ GeV. The dashed histogram is the expectation from signal MC events, normalized to the number of signal candidates in the selected region. The p_t balance requirement is indicated by the arrow.

code [11]. We generate 10^5 MC events for both e^+e^- and $\mu^+\mu^-$ decays of J/ψ , at nine different W points between 3.89 and 4.15 GeV. The efficiency for the signal process at $W = 3.92$ GeV is determined to be $(1.85 \pm 0.20)\%$ ($(1.26 \pm 0.14)\%$) for the $J^P = 0^+$ (2^+) assumption; the efficiency is defined for the range $Q^2 < 1.0$ GeV², for each incident photon. We assume production in helicity-2 for $J^P = 2^+$ [6] and decay to $\omega J/\psi$ in an S-wave for both 0^+ and 2^+ . The other two possible J^P assumptions, 0^- and 2^- , are similar and give an efficiency close to that for $J^P = 0^+$.

Based on the efficiencies calculated for the two J/ψ decay modes, the fraction of signal in the e^+e^- mode is expected to be 36%. This is consistent with the fraction in the data: 27 $J/\psi \rightarrow e^+e^-$ events among the 73 signal candidates.

Sources of systematic errors in the efficiency determination and their contributions are listed in Table I. We confirm that the inefficiency due to each of the particle identification cuts, (3) and (8), is very small, less than

TABLE I: Sources and sizes of systematic error in the efficiency determination

Source	Syst. error (%)
Trigger efficiency	2
Track reconstruction	4
π^0 reconstruction	3
Particle identification cuts	2
Effect of background hits	3
J/ψ selection	3
ω selection	6
W -dependence, effect of background, etc.	3
Luminosity function, integrated luminosity	5
Total	11%

1%, for signal events. The uncertainties in the efficiencies of the invariant mass cuts are estimated by varying the selection regions near $M(l^+l^-) = M_{J/\psi}$ and $M(3\pi) = M_\omega$ by $\pm 20\%$ in the MC. We sum the uncertainties in quadrature, and find 11% in total.

Treating the observed structure as a resonance denoted by $X(3915)$, we derive the product of the two-photon decay width and the branching fraction to $\omega J/\psi$, using the yield parameter N_R from the fit and the selection efficiency. We obtain

$$\begin{aligned} \Gamma_{\gamma\gamma}(X(3915))\mathcal{B}(X(3915) \rightarrow \omega J/\psi) \\ = \begin{cases} (61 \pm 17 \pm 8) \text{ eV} & \text{for } J^P = 0^+ \\ (18 \pm 5 \pm 2) \text{ eV} & \text{for } J^P = 2^+, \text{ helicity-2.} \end{cases} \end{aligned}$$

Based on this result, and the measured width Γ , the product of the two partial widths of the $X(3915)$, $\Gamma_{\gamma\gamma}(X)\Gamma_{\omega J/\psi}(X)$ is of order 10^3 keV². If we assume $\Gamma_{\gamma\gamma} \sim \mathcal{O}(1$ keV), typical for an excited charmonium state, this implies $\Gamma_{\omega J/\psi} \sim \mathcal{O}(1$ MeV): a rather large value for a charmonium-transition partial width of such a state. This value of the product of the partial decay widths is roughly compatible with the prediction assuming the $D^*\bar{D}^*$ bound-state model [5].

To conclude, we have observed a resonance-like enhancement in the $\gamma\gamma \rightarrow \omega J/\psi$ process with a statistical significance of 7.7σ , which contains $49 \pm 14 \pm 4$ events in the peak component. The mass and width have been measured to be $M = (3915 \pm 3 \pm 2)$ MeV/ c^2 and $\Gamma = (17 \pm 10 \pm 3)$ MeV, respectively. These values are consistent with those of the $Y(3940)$, which is seen in the $\omega J/\psi$ final state [3, 4], and close to those of the $Z(3930)$, which is seen in $\gamma\gamma \rightarrow D\bar{D}$ [6].

We thank the KEKB group for excellent operation of the accelerator, the KEK cryogenics group for efficient solenoid operations, and the KEK computer group and the NII for valuable computing and SINET3 network support. We acknowledge support from MEXT, JSPS and Nagoya's TLPRC (Japan); ARC and DIISR (Australia);

NSFC (China); DST (India); MEST, KOSEF, KRF (Korea); MNiSW (Poland); MES and RFAAE (Russia); ARRS (Slovenia); SNSF (Switzerland); NSC and MOE (Taiwan); and DOE (USA).

-
- [1] Belle Collaboration, S.-K. Choi *et al.*, Phys. Rev. Lett. **100**, 142001 (2008); Belle Collaboration, R. Mizuk *et al.*, Phys. Rev. D **78**, 072004 (2008); BaBar Collaboration, B. Aubert *et al.*, Phys. Rev. D **79**, 112001 (2009).
- [2] Belle Collaboration, K. Abe *et al.*, Phys. Rev. Lett. **98**, 082001 (2007); Belle Collaboration, P. Pakhlov *et al.*, Phys. Rev. Lett. **100**, 202001 (2008).
- [3] Belle Collaboration, S.K. Choi *et al.*, Phys. Rev. Lett. **94**, 182002 (2005).
- [4] BaBar Collaboration, B. Aubert *et al.*, Phys. Rev. Lett. **101**, 082001 (2008).
- [5] T. Branz, T. Gutsche, V. E. Lyubovitskij, Phys. Rev. D **80**, 054019 (2009).
- [6] Belle Collaboration, S. Uehara *et al.*, Phys. Rev. Lett. **96**, 082003 (2006).
- [7] S. Godfrey and S.L. Olsen, Ann. Rev. Nucl. Part. Sci., **58**, 51 (2008).
- [8] Belle Collaboration, A. Abashian *et al.*, Nucl. Instr. and Meth. A **479**, 117 (2002).
- [9] S. Kurokawa and E. Kikutani, Nucl. Instr. and Meth. A **499**, 1 (2003), and other papers included in this volume.
- [10] A small fraction of the data (87 fb^{-1}), from early in the experimental run, has been recovered from the event selection for a previous study [6]. The following requirements, unrelated to the present analysis, were applied: (A) there is no photon with energy exceeding 0.4 GeV in the event; (B) the net transverse momentum of the four charged tracks is less than 0.2 GeV/c. These conditions reduce the selection efficiency for the signal process to 50–60% of that in the main sample.
- [11] S. Uehara, KEK Report 96-11 (1996).